T.C.

ALTINBAS UNIVERSITY

Institute of Graduate Studies

Electrical and Computer Engineering

MINIATURIZED FLEXIBLE METAMATERIAL ANTENNA OF CIRCULARLY POLARIZED HIGH GAIN-BANDWIDTH PRODUCT FOR RF ENERGY HARVESTING

Malak ALAUKALLY

Master of Science

Supervisor

Asst. Prof.Dr. Doğu Çağdaş ATİLLA

Istanbul, 2021

MINIATURIZED FLEXIBLE METAMATERIAL ANTENNA OF CIRCULARLY POLARIZED HIGH GAIN-BANDWIDTH PRODUCT FOR RF ENERGY HARVESTING

by

Malak Naem Nashoor ALaukally

Electrical and Computer Engineering

Submitted to the Graduate School of Science and Engineering

in partial fulfillment of the requirements for the degree of

Master of Science

ALTINBAŞ UNIVERSITY

2021

The thesis titled “MINIATURIZED FLEXIBLE METAMATERIAL ANTENNA OF CIRCULARLY POLARIZED HIGH GAIN-BANDWIDTH PRODUCT FOR RF ENERGY HARVESTING” prepared and presented by “Malak ALAUKALLY” was accepted as a Master of Science in Electrical and Computer Engineering.

___________________________________	___________________________________
Prof. Taha A. ELWI Co-Supervisor	Asst. Prof. Dr.Çağdaş ATİLLA Supervisor

Thesis Defense Jury Members:

Asst. Prof. Dr. Çağdaş ATİLLA	School of Engineering and Architecture, Altinbas University	__________________
Assoc. Prof. Dr. Yasa Ekşioğlu ÖZOK	School of Engineering and Architecture, Altinbas University	__________________
Asst. Prof. Dr. Cahit KARAKUŞ	School of Engineering and Architecture, Istanbul Esenyurt University	__________________

I certify that this thesis satisfies all the requirements as a thesis for the degree of Master of Science.

Approval Date of Institute of Graduate Studies ___/____/____

I hereby declare that all information in this document has been obtained and presented in accordance with academic rules and ethical conduct. I also declare that, as required by these rules and conduct, I have fully cited and referenced all material and results that are not original to this work.

Malak Naem Nashoor Alaukally

DEDICATION

I would like to thank Allah Almighty for my success in my studies, my dear father and my teacher, leader and inspiration, my dear mother, my dear brothers, and everyone who stood beside me, I thank you very much .

ACKNOWLEDGEMENTS

First and foremost, all praises be to Allah subhanahu wa ta'ala (SWT) for his guidance and mercy in all my life.

Sincerest gratitude is to my advisor, Ass. Prof. Dr. Doğu Çağdaş Atilla, for his patience, guidance and his friendship during my graduate studies. I am proud having him as my advisor and mentor for my study.

I wish to express my gratitude to all my committee members for their support in this graduate work.

I gratefully acknowledge the I am forever grateful to my mother for her prayers, inspiration, faith and guidance during my life and study. All thanks to my father who helped me in becoming what I am today.

Also, I would thank my father for his ultimate support for his encouragements and I want to thank him for all the support he has given me during my life.

Finally, and most importantly I would like to give my warmest thanks to my friends and colleagues for their unconditional love and support.

God bless all of you.

ABSTRACT

MINIATURIZED FLEXIBLE METAMATERIAL ANTENNA OF CIRCULARLY POLARIZED HIGH GAIN-BANDWIDTH PRODUCT FOR RF ENERGY HARVESTING

Alaukally, Malak Naem Nashoor,

M.Sc., Electrical and Computer Engineering, Altınbaş University,

Supervisor: Asst. Prof. Dr. Çağdaş ATİLLA

Co-Supervisor: Prof. Dr. Taha A. ELWI

Date: 15/10/2021

Pages: 52

A discussion of using an Ultra-Wide Band (UWB) Hilbert-shaped Meta-Material (MTM) antenna structure for RF energy harvesting is exemplified in this article to conduct the use of organic substrates. Therefore, the proposed design is arranged as a low profile quadrangular MTM array in the context of wearable systems mounted on a prepared from an oxide of the Indium-Nickel composites mixed with a polymerized Palm fiber (INP) substrate. Ground plane of the antenna is constructed as a partial grand plane with array defecting an Electromagnetic-Band-Gap. In this study, fifteen samples of the INP substrates are prepared for the analysis. Additionally, the characterizations of prepared INP substrates are tested using a T-resonator transmission line technique printed on an FR4 substrate. In this technique, the measured scattering parameters are interpreted from two resonators with two different characteristic impedances to be employed for retrieving the relative permittivity (ε_r) and permeability (μ_r). This process is included to ensure the prepared substrates' properties controllability for manufacturing of microwave devices. After that, the proposed antenna is manufactured using a silver nanoparticles (SNP) printout. The performance of the proposed antenna is tested numerically and experimentally. The antenna performs an UWB response starting from 3GHz and extending over 10GHz. The measured gain spectrum shows four maxima peaks at 3.5GHz, 4.2GHz, 5.4GHz, and 6GHz with gain values of 1.1dBi, 2dBi, 3.4dBi, and 3.9dBi, respectively. Finally, the conversion efficiency of RF harvesting is measured experimentally for the antenna in case of flat profile and bended structure at the frequency bands of interest to reveal insignificant changes.

Keywords: RF harvesting, MTM, EBG, SNP, KNN

TABLE OF CONTENTS

Pages

<u>**Pages**</u>

LIST OF TABLES

Pages

LIST OF FIGURES

Pages

LIST OF ABBREVIATIONS

AI	:	Artificial Intelligence
IoT	:	Internet of Things
PAN	:	Personal Area Network
FSK	:	Frequency Shift Keying
TDMA	:	Time Division Multiple Access
OFDM	:	Orthogonal Frequency Division Multiplexing
RF	:	Radio Frequency
TLM	:	Transmission Line Network
FIT	:	Finite Integral Technique
FEM	:	Finite Element Method
GHz	:	Gigahertz
dc	:	Direct current
D	:	Density
SNP	:	Silver nanoparticles
AUT	:	Antenna under test
MUT	:	Material under test
L	:	Inductor
C	:	Capacitor
F	:	Frequency
G	:	Conductance
Go	:	Gain

BW	:	Bandwidth
H	:	Magnetic field
E	:	Electric field
Jc	:	Conduction current
Jd	:	Displacement current
R	:	Resistance
C	:	Speed of light
q	:	Charge

LIST OF SYMBOLS

μ	:	Mobility of electron
λ	:	Wave length
ω	:	Angle frequency
Zo	:	Characteristics impedance
S11	:	Return loss
S12	:	Transmission
$\tan\delta$	:	Loss tangent
σ	:	Conductivity
Θ	:	Zenith beam width angle
Φ	:	Azimuth beam width angle

1. INTRODUCTION

1.1 HISTORY

Micro-circles were used in the early middle where of the first half of the twentieth century to utilize the printed circuitries and the second half of the parallel circle wires. Furthermore, a new invention came in the second part of the same century, convincing the famous communication engineering research school to open the translation of the entire printed circuits [1]. Basically the matter of the precise condition could be attended from for the ground-plane to be transmitted to the actual frequency band, and then the use of an RF feed source mating processes [2]. It does not depend on the completeness of the atmospheric transmission; it does not reflect the line reflection from the almanac. The substance is given over to the person who can flip it inside out, which is the microstrip system, and who can use a radial picture to track the magnetic field as it increases in the five moons. [3] The idea of microstrip is the focus of the field introduction due to the fringing effects. In general, these structures radiate the electromagnetic fields in the broad side direction [2, 3]. Therefore, they were used in different urgent applications. For example, the actual GPS system was the topic of the creation of the microstrip aircraft at the time of publication, approximately 1974. However, it is not possible to place these long pieces in the mortgage confinement without industrial applications or trade due to the effects of excessive defects in the radiation to prevent harm [6]. This is until the fact that the damage is affected by the negative effect on the characteristics of the radiating light. In terms of time, power, and dread of the microwave oven, in addition to the sky, which is the waves of heroism from above, most of them do not perceive the resurrection in terms of time, power, and fear of the microwave oven. [3] In general, "the benefits of following and microstrip are in fact the benefits of axial transit and calligraphy," as stated in 1955 [5]. If you have any reservations about using the microstrip, try it right away.

The dispute can be delivered using the microstrip approach, but removing the limit from the exact removal with some high and mechanical characteristics of the essence of the concealed flaws is challenging. Deanlinger said in 1969 that the importance of observing the essence of exact circumstances in the shape of rectangles and rectangles may be regarded seriously. [6] In the past, if half of the amber penetrates and the radius of the radius may be transmitted, it was tightly bound. If the microstrip line is left open during the suspension, according to Deanlinger, the re-action and the ray's brightness, the eclipse will cause the eclipse to be deducted from the hero's waves in all places. It is well known that when the radiation is at its peak and is visible in the suspension, one half of the distance or the length of the repetition of the length is used. If the limit is surpassed, at least from the edges essence, to alter and sense the quantity of the patch edge ends from the unlocked surface waves. The ground plane may extremity height can be exceeded to the point where can be reached up to 70 degrees from the expanded arch. There is no scale for half-diameter radial vessels, which increases the likelihood of existence to seven and fifty half-diameter to half-diameter microstrip. Represent some of the advantages of microstrip air, such as the. In fact that it is one of the safest structures and can be embedded with electronic circuits. Materials to use on things other than spider webs and is free of scraping issues. If this shift is due to the fact that the microstrip is a significant refinement, it is critical that you have a big number of them in the early 1970s, followed by the line, planes, souls, and images and pictures, pictures, pictures, pictures, pictures. In general, the Howell line is a microstrip air rectangle that feeds the microstrip line. If the weather circumstances are favorable, the first to read poetry for the republic is in the days of the days. It draws a significant number of people from the sector to vote on the various options. And if it's tough to reach the eyeballs up to half their diameter, that's okay. The most likely growth is the multiplication of minor conditions, whatever is the lowest volume. There is little light in the morning because of the convenience of public administration in 1981 and microstrip air support, which makes IEEE microstrip air a special difficulty in IEEE climate and distribution services [7].

1.2 INTRODUCTION

People in the current days are treated with cutting-edge services such as wireless communication in real time. These are the electromagnetic wave propagation gadgets which surround the mechanical device assignment. The primary component of the system is open space. Since the invention of the antenna, the antenna has played an increasingly important role in human social life. It is an important radio device for transmitting and receiving electromagnetic waves and an important part of the radio communication system. The performance of the antenna will directly affect since the invention of the antenna, the antenna has played an increasingly important role in human social life. It is an important radio device for transmitting and receiving electromagnetic waves and an important part of the radio communication system. The performance of the antenna will directly affect the quality of the communication system. In order to improve the efficiency and performance of antennas, modern communications have paid more and more attention to the study of antenna multi-band miniaturization performance [1-2]. The quality of the communication system can be enhanced by conducting novel antenna designs. In order to improve the efficiency and performance of antennas, modern communications have paid more and more attention to the study of antenna multi-band miniaturization performance [1-2].Since the invention of the antenna, the antenna has played an increasingly important role in human social life. It is an important radio device for transmitting and receiving electromagnetic waves and an important part of the radio communication system. The performance of the antenna will directly affect the quality of the communication system. In order to improve the efficiency and performance of antennas, modern communications have paid more and more attention to the study of antenna multi-band miniaturization performance [1-2].

Imitating the classical grille structure multi-band antenna, combining the unique structure of the classic grille with the theory of antenna design, the changeable pattern inside the grille can make the antenna have multi-band performance characteristics. By changing the structure of the window grille, the influence of its structure on the antenna performance is analyzed, and the structure that makes the antenna performance the best is found [3].Background of the Study.

Multi-frequency band technology is to increase the path through which current flows on the surface of the radiator to generate resonance and realize multi-frequency bands. The current multi-band implementation technologies include: multi-patch technology, slot loading technology, multi-branch structure, fractal structure, and so on. By adding one or more patches, the radiator can work in different resonant modes, thereby generating multiple resonant frequency points to form a multi-band antenna [5-6]. Open one or more slots on the surface of the radiator to extend the path of the antenna surface current, change the path of the surface current, and make the radiator generate multiple resonance frequencies [7-9].The antenna adds branches to the radiator, and uses electromagnetic coupling between the branches to generate multiple frequency points [10-

12].Using the self-similarity of the fractal structure, after a certain number of iterations, each part of the radiator corresponds to a different resonance frequency to achieve the multi-band performance of the antenna [13].

Due to its practical capabilities in wireless power systems, RF harvesting technology based on UWB programming has recently caught [2].the attention of academics in a major way [1]. As a result, [2].major advancements in Internet of Things (IoT), wireless and wireless devices, 5G networks, wireless sensor networks, and remote sensing ports have been made [2]. This is because most portable gadgets that rely on batteries for their performance still have a different solution [3]. However, when used on PCB devices, such technology faces substantial problems due to high conversion efficiency (r) [4and restricted microstrip antenna limitations [3]. Furthermore, the unrestricted usage of batteries [4contributes to the environmental problem [4]. As a result, replacing outdated technologies with RF for the management [5] of stored green solutions is no [5] longer a pressing necessity [3]. To decrease [5] intersection junctions between circuit monopoles printed on MIMO systems [5] and to gain bandwidth improvements [6, ring resonators [5] are separated. Another technique, utilizing the fractal [8] form MTM, was presented in [7] to minimize the interactions between the [8] horns in the MIMO series. [8] Developed EBG [8] faults in incomplete global airplanes to increase bandwidth. To increase bandwidth, another antenna based on the MTM and EBG structural combination was proposed [9]. To enhance Wi-Fi bands, [11] comparable MTM components with [11] a dipole antenna have been introduced [10]. The authors [11] built on their previous work by include the effects of MTM installation in the antenna patch of [11] portable Wi-Fi systems. The printed construction of the monopole antenna-based [11] MTM with distant sensing applications [11] is based on [12]. Different research programs [13] describe a number of cylindrical-based EBG problems. MTM and EBG frameworks [14] - [20] were later suggested to indicate RF-strength. In satellite health monitoring systems, for example, the authors in [14] employed an MTM-based antenna configuration to gather microwave power. A multiband EBG antenna for microwave harvesting was proposed by the authors in [15]. The MTM based on a UWB monopole has been utilized to gather RF power across several groups [16]. At [17], RF was harvested in two frequency bands using a flexible MTM antenna. A cylindrical MTM antenna for RF power harvesting was suggested in [18]. [20] Energy harvesting discusses organic substrates based on UWB MTM antenna. Previous research, on the other hand, has not looked at the impact of material loss on harvest performance. Furthermore, in terms of RF power harvesting, the optimum approach to decrease such losses has yet to be explored.

1.3 MOTIVATION

Due to the need for an unexpected increase, then the expansion of the room with new teeth in the diversion system, as well as the one who was accustomed to the inner courtyard. And the purpose of preserving this vision is to simplify the need to take advantage of the air sufficiently and to gain and the breadth of the word that will be suspended on the plane. Discussion of this method until a new location is developed to find the course of time, and it is possible for a person to be able to use the technology of eating and eating at night. In addition, it is possible to see the shape of the pattern in the air in front of the part of the pulse, but in that part of the natural decline of the imitation of the constrained theories of congestion.

1.4 RESEARCH PLAN

The antenna is printed with SNP ink on a flexible INP substrate to enhance the gain bandwidth product over the frequencies from 3GHz and extend over 10GHz. The MTM unit cell is structured as a fractal Hilbert curve of a certain width to provide SNP conductor attenuation factor similar to the attenuation factor of copper. An extensive analytical study based on KNN algorithm is reported to illustrate the best method to enhance the INP substrate for the proposed design. For this, fifteen INP substrates are fabricated and tested with T-resonator printed on FR4 substrate. The RF harvesting conversion efficiency is measured when the antenna placed as a flat structure and bent over cylindrical objects based DC rectifier circuit.

1.5 PROBLEM STATEMENT

In the last few decades, the need for novel green energy resources for self-powered wireless applications has attracted much attention and grown significantly. This interest has been coupled with the importance of controlling the data collection and positioning navigation surfaces. Nevertheless, the most important need is the national borders security against smugglers on both land and sea. Therefore, monitoring such surfaces in real time is not an easy matter with all these input parameters that complicate the compromising point of view as each parameter is an effective part by itself and highly important to figure out. All these requirements motivated the researcher to investigate and develop a low cost, low profile, light weight, and an antenna structure that can be integrated into solar panels in a self-powered wireless system.

1.6 RESEARCH OBJECTIVES

In light of the problem statement presented above, the main research objective is to investigate and develop a low cost, low profile, light weight, and an antenna structure that can be integrated into solar panels in a self-powered wireless system.

They are devices that use energy from external natural/ non-natural sources which can be captured and stored. There is a need for such system because:

I. there can be sufficient power as and when it is needed,

II. It will offer l long lifetime with little or no maintenance,

III. It is easily and cheaply installed,

IV. It offers flexibility.

RF and microwave energy are among the external non-natural sources that can be captured and used to power the electronic systems of wireless sensor nodes. Therefore, it is the subject of this research to develop a microstrip antenna based on a printed circuitry to receive and transmit the collected data by the sensor node and at the same time to be used for harvesting the RF and microwave energy.

1.7 RESEARCH CONTRIBUTIONS

To overcome the antenna limitations, a fractal printed circuit antenna is proposed in this research to show the following advantages:

I. The fractal geometry shows excellent size reduction in comparison with other techniques by increasing the current path within a limited area,

II. Fractal antennas provide multi-bands at different frequency resonances,

III. Such structure may be a subject for providing a wide band,

IV. The antenna gain of fractal geometry can reach excellent enhancement in comparison with traditional antennas.

1.8 SIGNIFICANCE OF THE STUDY

I. By using air correction, if the tongue of the tongue assumes that it conforms completely to the engineering of hesitation and / or that if it is formed from the shape of the material exchanged, then the matter is abandoned so that the one who has the right to do so will take action,

II. The antenna will be designed and simulated using different commercial software packages including CST MWS and HFSS,

III. Perform the related electronic circuits including the A/D converter, the battery charger, the matching circuits and amplifiers,

IV. Fabricate the antenna structure and integrate it into the related electronic circuits then test the performance,

V. Measure the harvested power in real outdoor environments.

1.9 SCOPE AND LIMITATIONS OF THE STUDY

The address of the corpse of the besieger in the conductor of the air to the industrial engineer is cut in such a way that it is suitable for him to hold it firmly in the distance in half the diameter of the movement of the path of the corpse when it is in a hurry. Lastly, the theme of the ending is in the form of persuasion from the study of the distilled plane with the assignment CST-MWS from the completion of the course of all antenna feature courses. However, the unified atmosphere is based on the fraction of Hilbert in the rectangular geometry based on the third order with EBG defects.

1.10 ORGANIZATION OF THE THESIS

This thesis comprises five chapters. Chapter 1 investigates and analyses numerical studies of the photovoltaic technology impact on integration of the microwave terminals as described in Chapter 2, with the focus on met materials and antennas separately. In this work, the electromagnetic characterizations of the met material structures are the method used to compute the relative permittivity and permeability, which are investigated. Nevertheless, the antenna performance in terms of a single terminal is evaluated. Chapter 3 investigates the implementation of the antenna structure according to meet materials. The effect of the antenna array with and without met material structure is developed to realize the optimal antenna performance with regard to bandwidth and gain enhancement. The integration and fabrication of the antenna structure based on met material structure is shown chapter 4. Chapter 5 concludes the study and makes recommendations for future related work to be considered.

2. THEORY OF MICROSTRIP PATCH ANTENNA

2.1 MICROSTRIP ANTENNA

In essence, it is established from specific situations in the plane of the conquest of the soul (as in the case of a wave in the region of the dragon region), it creates unity in the sense of feeling. On the one hand, from the other side, he is on the right track. Using healthy nerves and gold in mineral mines. There is a correction of the structure in which it is built, because it does not use a simple situation to correct the line by looking at flat words and a simple pattern is an example of analyzing the position of the person who looks at it. Square, rectangle, polar curve, triangle, elliptical shape, circle with certain basic shapes. Circular shapes and quadrupeds and poles are the most common types of work, and are arranged according to their order in analysis and art. It is necessary to publish amber waste items with evidence of extraction $2.2 \leq \leq 12$ [8]. Mouth play is important for normal air signals in the zero class $.003 \leq h \leq 0.05$.

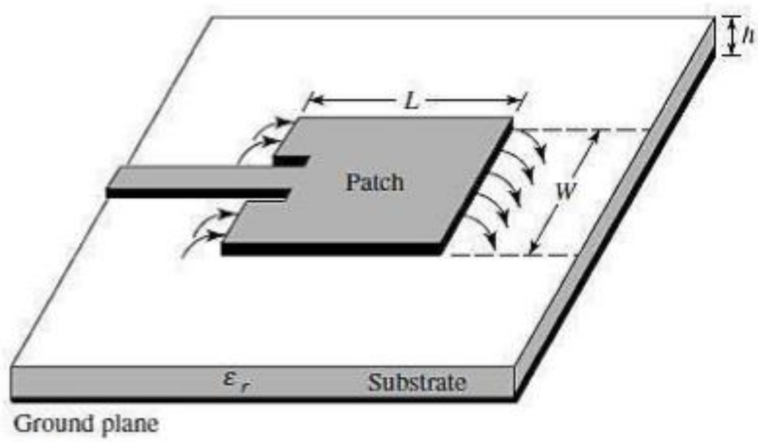

Figure 2.1: Microstrip patch antenna.

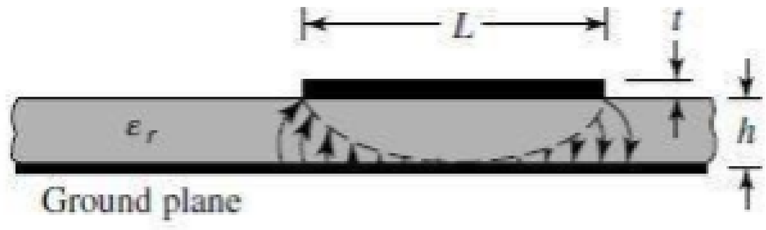

Figure 2.2: Side view of the microstrip antenna.

It means the waves of the Microstrip air from the width of the movement. However, in my opinion, the fact that the number is at least from the line as the interference is important, if it is the property, microstrip air is useful. Width of microstrip transmitters without delay equal to the surface of the surface [4]. What some basic strategies do you hesitate to do [12]. The view of the unity of unity and the second rule [9]. The airwaves are not always a hadith with the characteristics of the airwaves, but the airwaves are mixed with the message and the airwaves. In the ordinary, do not test the child by entering the microstrip air, and do not let the returnees send the true message (50 days review). It is permissible for the designer to do so until the surface waves deceased and the cause of the no effects of the transmission line at the edges of the substrate. There is another way to overcome this problem, and it is to create strong networks like the one that exists between the antenna and the line of transmission. If there are a number of ways to match the required power with the antenna structure, then the theory of the circle with the justification of the match.

The building method is used to modify the structure of the ground plane, and it is different and similar. If the curves of the patch structures curves are hardened from the edge of the survey, they do not have the intention in the performance and the factors of the murder. In addition, a diverse set of afflictions by the way of employing the citrus that is in it is affected by the body, the unfavorable land, the perception of the details, and the construction of the transmission line for hesitation is the question of the exact line. From the limit of the orderly atmosphere, the designer can make the antenna register easily by using radiant and polar arrays. It is easy to microstrip the antenna with forcing the formation of the natural shape and the movement of the radiation in a certain direction which adds weakness like the bath in three dimensions, therefore varying the capacitive value would a good solution.

The antenna gain can be described directly from [1] using the empirical formula as:

$$Go = \frac{30,000}{\theta\varphi} \tag{2.1}$$

The antenna reflection coefficient can be evaluated as:

$$\Gamma = \frac{Zo-Za}{Zo+Za} \tag{2.2}$$

Therefore, S11 can calculated from

$$S11 = 20 \log (\Gamma) \tag{2.3}$$

2.2 RADIATION MECHANISM

In the general public 1969, the signals of the tenant are drawn to the fact that if the microstrip line is left open, it will not be extended and added to the other side of the body for the force from the side of the body, with the exception of one from the other side. The wisdom of the sick means that the amount of the arc originates from the larger region, especially between them. The sincerity of the believers, even if it is spread over the course of following the revelation, is due to the words of those outside the commentary. With the knowledge of the existing equipment behind half the diameter of the microstrip air, look at the square air with a length of 1/2 that forms the microstrip arc line. What is possible is the realization of the correctness of the rectangular flow lines, the microstrip line, and the opening is open on one side and the application of the conditions on the other side. In fact, it is true that the lamp is half the length of the window and it opens with different branches, so it is necessary to have the current date in the angles of the moment (beginning and end) of the moment zero and in the moment of the moment. And what is possible is that in the age of hadith and narration around the environment, the degree of extinction is outside this error. It is possible that the wall of heroism is strong in the beginning, seriously and seriously through the number of blessings [9].

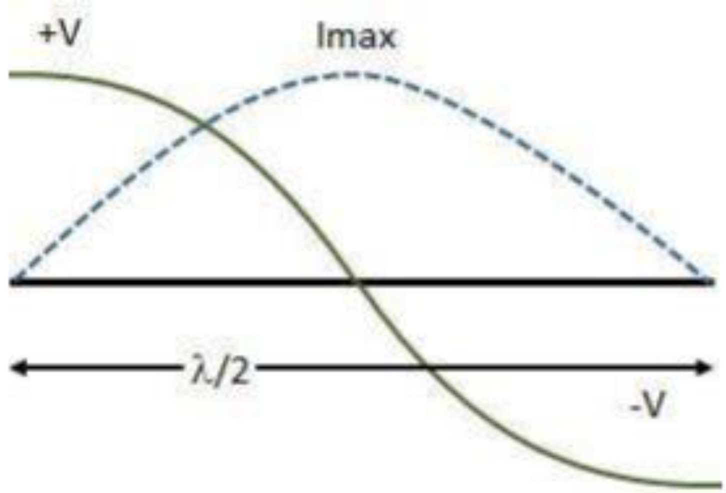

Figure 2.3 Current and voltage variation along the patch.

The distribution of the power of the title field next to the clip is the same as the parent proof below. Sector issues are below the point where the nook is referred to as opposed to directing. These disciplines do not suddenly stop the ant from stopping. In the corners photography fields are being constructed and sector issues are in the bow position. In addition the frying field absorbs the rays. Therefore, those fringing is the cause behind the rays from the microstrip antenna.

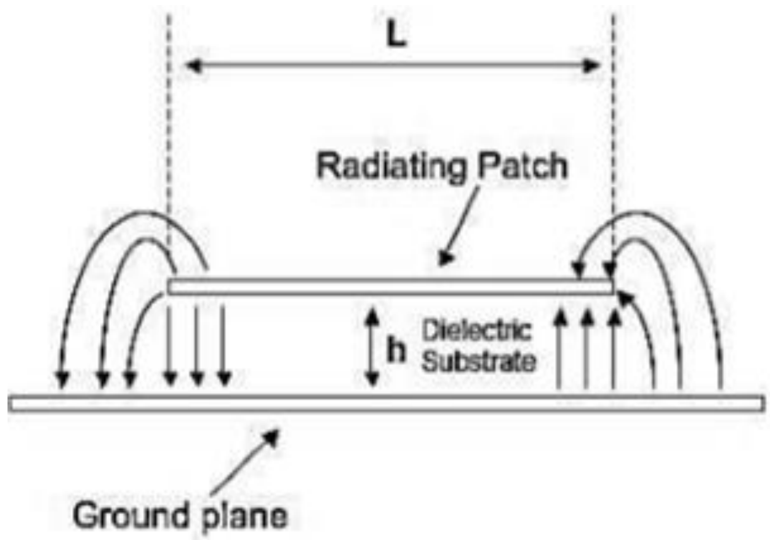

Figure 2.4: Field fringing on the antenna patch.

2.3 ADVANTAGES AND DISADVANTAGES:

Microstrip antenna is a low-cost antenna with low weight and may be extremely smooth in installation because it is popular for mobile wireless gadgets that include cell phones, pagers and other efficient chat facilities including satellite tv for pc, missile, space, aircraft and so on. A number of outstanding benefits of microstrip antenna as mentioned by Randy Bancroft [3] and Garg [10] are given below:

I. Contrary to the commitment of the industry and its obligations.

II. It is possible to cultivate without problems in any place.

III. What is possible is the action of what is created by the longest possible correction.

IV. What is possible is to limit the difference between the problems with the preferred season.

V. Strong, persistent, resilient and resilient.

VI. Suitable for complete microwave ovens (microphones).

VII. The height of the soul and the power of attorney in the angles can be a problem.

From the other region, the microstrip air currents are related to the major factors and constraints when compared to other regions. Some microstrip desks are mentioned above:

I. Consolidation of distances.

II. Adequacy of polarity.

III. I mean the illumination of that weak.

IV. I can reduce the width of speech with resistance (from 5 10 to 10 % on the way)

V. Distinguished losses in waste, materials and products.

VI. Sensitive to natural contents such as heat and moisture.

There are countless customs to overcome this problem, the bandwidth of the microstrip antenna can vibrate using certain unique techniques such as inefficient flight techniques, dense spots, split spots, parasitic patch. The gain and power of antenna handling can be enhanced by making an antenna list. The use of electromagnetic band gap (E_{Bg}) and metamaterial structure also has implications within the development of antenna signals [20].

2.4 APPLICATIONS

Behind some limitations due to several advantages the microstrip antenna has been found to be useful in different systems. Microstrip antenna is widely used within defense systems such as arrows, planes, satellites and rockets. Now-day microstrip antenna is used in the industrial sector because of its low cost and smooth operation for profit in the form of printed circuit generation. Due to the enlargement and ongoing research within the microstrip antenna area it is estimated that in the near future most of the traditional antenna will be replaced with the help of a microstrip antenna. Some of the most advanced microstrip antenna packages are:

I. Mobile wireless-communicant,

II. Satellite Communication,

III. Global Positioning System,

IV. Direct Broadcast Satellite System,

V. Antenna for Pedestrian,

VI. In Radar Applications,

VII. Application in Medical Science.

3. THEORY OF THE PROPOSED WORK

In this work, an extensive study based one experimental and analytical calculations, the authors explored a method for dielectric and conductor losses reduction. For this, a flexible miniaturized MTM based antenna patch width defected ground plane is designed for RF energy harvesting applications. The proposed antenna covers the frequencies of UWB devices and wireless communications systems including cellular networks or 5G applications.

3.1 SUBSTRATE PREPARATIONS

The INP substrate is prepared from organic materials of palm trees where they are rich with cellulose fiber [17]. These fibers are produced from crushing the palm leaves to 100µm particles. The produced powder is washed with hot water and dried inside a convection oven for 120 minutes. To remove the wax leftover in the created powder, acetone washing path is conducted. Then, the prepared powders are mixed with poly-ethylene and nickel nano-partials. The manufactured substrate samples from varying the mixture ratios randomly are listed in Table 3.1. The authors considered these models randomly to be used in their test process as will be seen later.
Each sample is mixed using a blending machine under 180°C temperature for 30 minutes. The prepared substrates are pressed to be shaped as square layers with 2mm thickness. Therefore, to ensure surface smoothing with minimum air gaps, the pressing time is carried out for 10 minutes with three different pressure rates to each sample as: 90kg/cm^2, 115kg/cm^2, and 130 kg/cm^2. Therefore, three times each model is pressed with 1 hour waiting period. It is concluded from the table 3.1, the used sample of nickel ration is less to avoid the conduction losses.

Table 3.1: Prepared INP samples

Mixture ratio			Sample name
Poly-ethylene/ g	Palm tree fiber/g	nickel nano-partials/g	
65	34	0.1	1
69	41	0.3	2
75	46	0.5	3
81	49	2	4
87	52	1.0	5
91	55	1.2	6
94	59	1.4	7
99	62	1.6	8
105	69	1.9	9
105	71	1.5	10
100	77	1.1	11
109	63	0.5	12
70	55	1.3	13
88	39	1.7	14
111	45	0.8	15

3.2 SUBSTRATE CHARACTERIZATIONS

Now, a transmission line structure of T-resonator is fabricated on an FR-4 substrate with two different dimensions to provide two different characteristics impedances 50Ω and 30Ω as explained in [13]. The authors designed their T-resonators to ensure the first resonance mode (f_o) is located around 1GHz, and the other modes increase harmonically up to 10GHz. The fabricated transmission line is used to retrieve ε_r and μ_r values from the S-parameters. Consequently, the proposed sample models are experienced practically to estimate the S_{12} and S_{11} parameters using

PNA8720 vector-network-analyzer. The resonances of S_{12} response of the suggested structure without samples (in air) are considered the reference cases. Formerly, after filling the structure with the itemized models in Table 3.1, the measured S_{12} response are presented in Figure 3.1. The obtained S_{12} results are categorized to three dissimilar collections as gotten in Figure 1. The organization is done according to the resonance change in-comparison to the original T-resonator before presenting the INP models. For this, group_1 denotes samples with no significant changes in the resonances, group_2 is reflected for the models lead frequency-shifts, and group_3 is for the models with delay frequency-shifts. In the sense of that, the authors spend their process to identify the best samples for their application to realize maximum antenna size reduction with minimum losses. This requires a substrate with highest ε_r and μ_r but with minimum material losses. Therefore, the author selected group_3 that shows more promising candidate due to the lagging in the frequency shift as will be seen later.

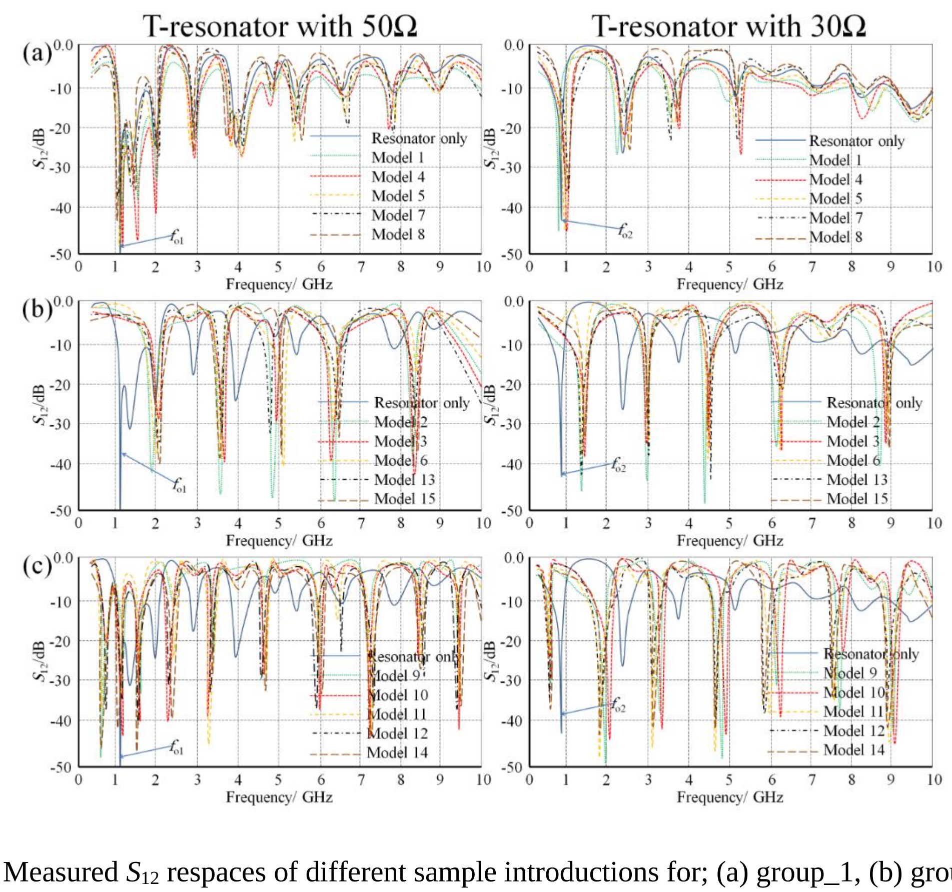

Figure 3.1: Measured S_{12} respaces of different sample introductions for; (a) group_1, (b) group_2, and (c) group_3.

From Figure 3.1, it can be seen that the fundamental frequency resonance (f_o) of the T-resonator is 1.1GHz. After calcification, it is observed in Figure 3.1(b) that f_o shows no significant change after introducing the samples from group one. However, it is observed in Figure 1(b) after introducing the samples of group two, f_o is mostly shifted with same band up to 2GHz. While, the frequency-variation is changed back to 0.5GHz, after using the group_3 samples to resonator. Therefore, the resonances-variations at different modes number (N) from the T-resonator (f_{Rn}) with respect to the nearest neighbor mode in the relative sample under test [6], (f_{sn}) is evaluated from Eq. 3.1 [6]:

$$\Delta f_n = \frac{\sqrt{\sum_{i=1}^{N}(f_{Rn}-f_{sn})^2}}{M} \tag{3.1}$$

where, M is the number of samples and in our case is 5 sample for each group. It should be noted that the calculated values difference (Δf_n) are computed from S_{12} response for each group as shown in Figure 3.2(a). Later, the variations in the magnitude of S_{12} response (ΔS_{12}) with samples introduction are evaluated. Therefore, the average differences in the T-resonators S_{12} magnitude (S_{12Rn}) with respect to S_{12} after sample introduction (S_{12s}) at each type is intended [5] rendering to the resulting:

$$\Delta S_{12n} = \frac{\sqrt{\sum_{i=1}^{N}(S_{12Rn}-S_{12sn})^2}}{M} \tag{3.2}$$

This is taken into account in our calculations to assess the effects of asset losses that often bring predictable components of ε_r and μ_r.

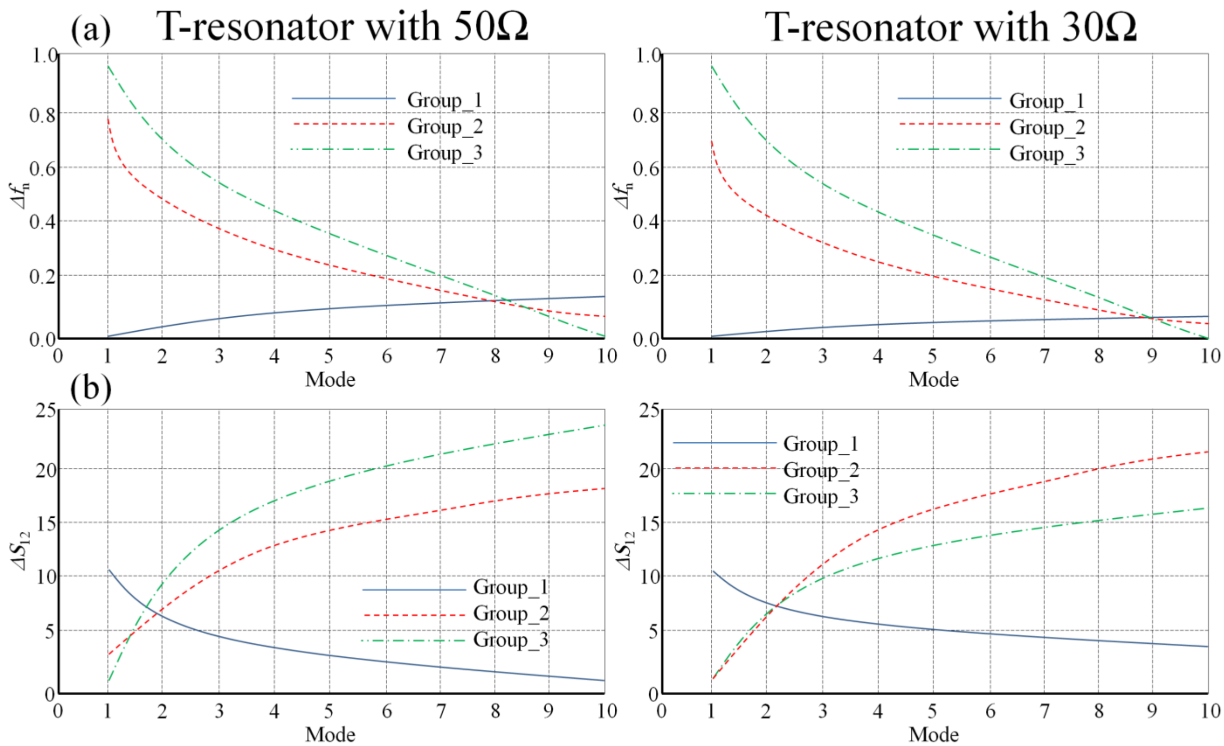

Figure 3.2: Average differences at different modes for each group; (a) Frequency resonance variation from S_{12} response and (b) S_{12} magnitude variation.

In overall, Figure 3.2(a) shows the core deviation in Δf_n can be observed in group_2 and group_3 is negative with the mode number rise. However, the variation in group_1 is pointed out almost insignificant with a constant slop from both T-resonators. Similarly, the changes in relative to ΔS_{12} increases with the mode number increase for group_2 and group_3 as seen in Figure 3.2(b); while, the changes in ΔS_{12} for group_1 are found almost constant.

Now, from the guided-wavelengths λ_g that is related to the length of the stub length (L) [6] of the T-resonator at the frequency-modes that can be intended [6] as:

$$L + \Delta L = \frac{[2(N-1)+1]\lambda_g}{4} \tag{3.3}$$

where

$$\lambda_g = \frac{c}{f_{rn}\sqrt{\varepsilon_e \mu_e}} \tag{3.4}$$

Therefore, by substituting Eq. 3 in Eq. 4, the resulted relation is given by:

$$\sqrt{\varepsilon_e \mu_e} = \left[\frac{(2N-1)c}{4f_{rn}(L+\Delta L)}\right] \quad (3.5)$$

To calculate material-losses, quality-factors (Q_L) are measured from the loaded T-resonators at 3dB from the dip of S_{12sn} response at the resonance frequencies in comparison to the unloaded quality factor (Q_u) [7] that is expressed as:

$$Q_u = \frac{Q_L}{\sqrt{1-(2)10^{((S12Rn-S_{12sn})/M10)}}} \quad (3.6)$$

However, the total attenuation loss is related to Qu [7] as:

$$\sqrt{1-|S_{11sn}|^2-|S_{12sn}|^2} = \alpha = \frac{8.686\pi f_r\sqrt{\varepsilon_e\mu_e}}{cQ_L} \quad (3.7)$$

Based on a neural network of K-Nearest Neighbor (KNN) algorithm that is adopted from [21] with input measurements, the relative values for ε_r and μ_r are retrieved.

Now, as explained later, the INP substrate usually consists of three elements (poly-ethylene, palm tree fiber, and nickel nano-particles) mixed with different values. Therefore, to evaluate the effects of each material introduction on the INP mix as a whole and the extent of the merging effects between these elements in one entity, the authors decided to find the first element of each curve in Figure 2. Therefore, this needs to be called a second polynomial curve equal to the acceptable assumption process for obtaining measurement function on the measured outcomes in Figure 3.2 as set out in Table 3.2. From the calculated results, it is found that the models in group_3 are more promising than other groups, with a variation of about 0.5% in the 12S12 values, which provides minimal reduction results. However, the complete diversity in that group according to Δfn is found in about 23% providing hope that ε_r and μr are greater than unity. The calibration equations in table 3.2 shows insignificant variation in the stander deviation due to the low effects of the nickel oxide introduction effects.

Table 3.2: Calibration equation and mixture percentage effects.

Case	Curve	Group Number	Calibration Equation	Mixture Percentage Effects
50 T-resonator	Δf_n	Group_1	$=0.1M^2-0.04M+0.22$	20%
		Group_2	$=0.65M^2-0.21M+0.1$	16%
		Group_3	$=0.8M^2+0.34M+0.3$	21%
	ΔS_{12}	Group_1	$=9.5M^2+4M+9.5$	21%
		Group_2	$=2M^2-2M+22$	50%
		Group_3	$=3.5M^2-0.04M+20$	0.5%
30 T-resonator	Δf_n	Group_1	$=0.2M^2-0.3M+0.7$	75%
		Group_2	$=.65M^2+0.21M+0.3$	16%
		Group_3	$=0.8M^2+0.37M+0.6$	23%
	ΔS_{12}	Group_1	$=8.5M^2+4.6M+10$	-27%
		Group_2	$=2.4M^2-2M+19$	42%
		Group_3	$=6.5M^2-0.4M+23$	3%

Based on Eq. 2.5 that is invoked to the Nicolson-Ross-Weir analysis in [5], ε_r and μ_r values of the proposed samples in group 3 are evaluated in terms of real and imaginary as listed in Table 3.3. From the listed results, the authors decided to pick model 11 for their antenna design that shows minimum imaginary parts of ε_r and μ_r with highest real values. The obtained results ensure that the effects of the obtained losses is reduced significantly from the nickel introduction.

Table 3.3: Electromagnetic characterizations of the selected models.

Model number	Re(ε_r)	Re(μ_r)	Im(ε_r)	Im(μ_r)
9	2.918	1.321	0.0025	0.019
10	2.583	1.433	0.0672	0.008
11	3.106	1.548	0.0451	0.013
12	2.781	1.572	0.0981	0.091
14	2.133	1.442	0.0783	0.898

4. ANTENNA DESIGN METHODOLOGY

Now, the antenna design is inspired Hilbert curve MTM [6], see Figure 4.1(a), to provide multi resonances at different bands. The antenna patch is structured from planar MTM array printed on the fabricated INP substrate. The individual MTM unit cell is coupled to capacitively to a T-shaped matching circuit as seen in Figure 4.1(b). To provide minimum conductor losses, the unit cell effective area is printed with narrow traces. Therefore, the maximum radiation efficiency could be achieved. This is discussed through the following mathematical analysis that starts from the conductive skin depth (δ) [8]:

$$\delta = \frac{1}{\sqrt{\pi f \mu \sigma}} \tag{4.1}$$

Therefore, the surface resistance (R_S) the printout for a given trace width (w) can be calculated from the limit below when $t/2\delta$>>1 [10]:

$$\lim_{t/2\delta \to \infty} (R_s) = \frac{l}{2w\sigma\delta} \frac{1}{\left(1 - e^{-t/2\delta}\right)} \approx \frac{l}{2w\sigma\delta} \tag{4.2}$$

In such case, the antenna radiation efficiency (e_r) is significantly affected by R_S as can be seen from the following relation [9]:

$$e_r = \frac{R_r}{R_r + R_L} \tag{4.3}$$

where, R_L is the combination of the conductor loss that is described the R_S and dielectric loss which is given by the imaginary parts of ε_r and μ_r as discussed previously. It is clear from Eq. 4.4 and 4.5, the thickness of the print out and the substrate μ is a dominate factor on the antenna efficiency. Therefore, choosing the substrate from the proposed models in group 3 is an important factor to achieve maximum e_r from the proposed antenna. Nevertheless, the value of w is another important parameter that realizes a significant factor as given in Eq. 4.4 on e_r through R_L component. However, increasing the trace width must not to go beyond the traces cross lines limitation in the proposed design. The proposed patch is excited with a 1.6 mm wide transmission line as presented in Figure 4.1(a). The ground plane is defected partially with 7×6 periodically EBG layer to enhance the radiation patterns of the antenna to be mostly omni directional radiator. Nevertheless, the EBG slot location is placed under the T-stub directly to improve the antenna coupling. Such enhancement could be achieved due to the field fringing magnification from the T-stub in both *E*- and *H*-field components through the substrate relative properties ε_r and μ_r multiplications [4]. Now, according to the result that is given in Eq. 4.4 and the fact of R_L increase is relative to the fringing leakage from radiators that can be expressed as radiation field losses from transmission lines as [6]:

$$\alpha_{rad} = \sqrt{\frac{\varepsilon_{re}\mu_{re}}{\varepsilon_r\mu_r}}\frac{0.42}{K(k)K\prime(k)}\frac{w^2}{\lambda_g^3} \tag{4.4}$$

where, ε_{re} and μ_{re} are the effective constitutive parameters, w is the print out width, λ_g is the guided wavelength, K is the complete elliptic integral of the first kind as a function (k) and given by [10]:

$$k = S/(S + 2w) \tag{4.5-a}$$

$$K' = K\sqrt{1 - k^2} \tag{4.5-b}$$

where, S is the space distance between each two printout traces. It is important to mention that, with four point technique, the electrical conductivity is measured for the printout using Keithley electrometer. It is found that the electrical conductivity is about 9.2±0.2×10^{4}S/m to be used in CST MWS and HFSS simulation process.

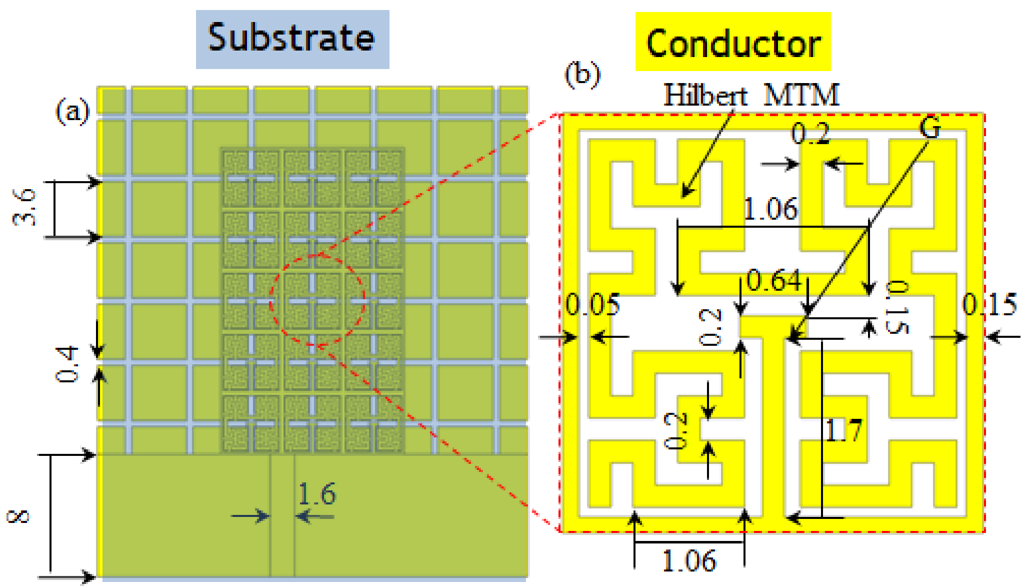

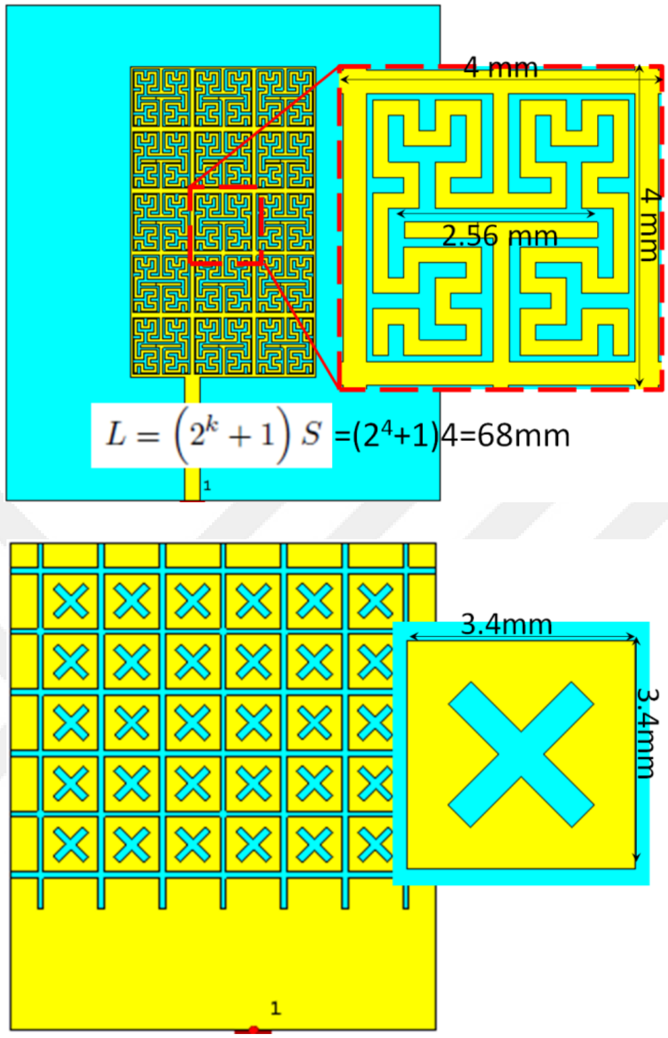

Figure 4.1: Antenna geometrical details in mm scale; (a) front view and (b) MTM unit cell.

In this section, it is developed a procedure based on Eq. 4.5 that is considered to arrive at the best width for the printout traces on the proposed INP substrate in comparison to the same printout on an FR-4 substrate. Therefore, two coplanar waveguide transmission lines are printed on the INP substrate one based on SNP and the other based on copper of the same dimensions. The radiation loss variation given by α_{rad} is calculated as seen in Figure 4.2(a) for the two transmission lines. The resulted attenuation variation with width change for the particular transmission lines is found to be intersected at a certain point. Therefore, such intersection reveals that at this particular point, the radiation losses from the two printouts on the considered substrates are the same and independent of the patch material conductivity, hence, the authors considered that in their design methodology.

To give the complete picture of the invoked analysis, the MTM on the patch, see Figure 4.2(a), is constructed as Hilbert shaped of the third order with lines printout according to the recommendations in [5]. To ensure that the driving current excites each unit cell in the proposed patch, the coupling gap (*G*) in Figure 4.2(b). However, keeping the input impedance of the proposed antenna around 50Ω and 0Ω over an UWB band for the real and the imaginary parts, respectively, the authors conducted a parametric study on the gaps between the Hilbert structure and the T-stub as seen in Figures 4.2(b) and 4.2(c). For this, the values of *G* are changed periodically in the MTM unit cells to improve the impedance bandwidth (Z_{BW}) by increasing the gap distance between (0.05mm up to 0.25mm) according the previous discussed criterion. This is considered in order to provide maximum coupling between the proposed antenna and the RF rectifier circuit.

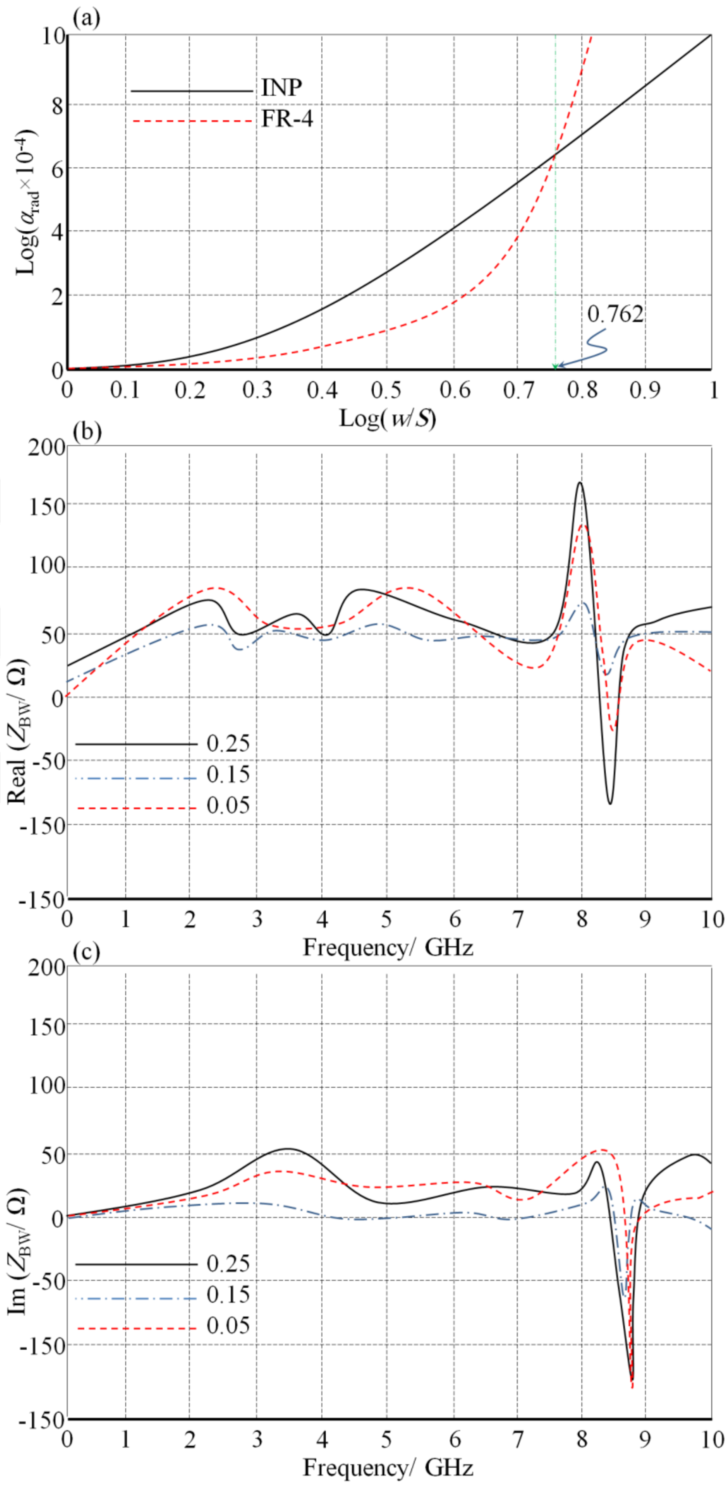

Figure 4.2: Effects of the printed traces dimensions on antenna performance; (a) *w*/*S* variation effects on the radiation losses, (b) and (c) the impedance response variation with G change on the INP substrate only.

It is observed that *G* variation has significant effects on the real part of the impedance matching values as seen in Figure 4.2(b) to be fluctuating around 50Ω for the real part in frequency range from 2.3GHz up to 8GHz. Moreover, the imaginary part of the impedance matching is found close to zero in the most frequencies of the same range as can be seen in Figure 4.2(c). The impedance response for three different G values: 0.05 mm, 0.1 mm, and 0.15 mm are compared to each other. It is found from the comparison that the *G* value with minimum impedance variation is when *G*=0.15 mm. Therefore, the principle of operation of the proposed MTM and EBG structure is discussed in this section. Basically, the method used in this work to enhance the antenna matching and gain can be explored from the dispersion diagram of the proposed MTM and EBG structures as in Figure 4.3(a). A low attenuation along the patch width is observed, while, the wave propagation along the patch length faces higher attenuation. Hence, the proposed unit cell is anisotropic EBG structure which allows controlling the length/width ratio without changing their physical lengths. The antenna gain spectrum change with the MTM and EBG inclusions introduction to the antenna structure is presented in Figure 4.3(b). It is found that the proposed MTM and EBG combination shows maximum gain enhancement due to their significant effects on the surface wave reductions [14].

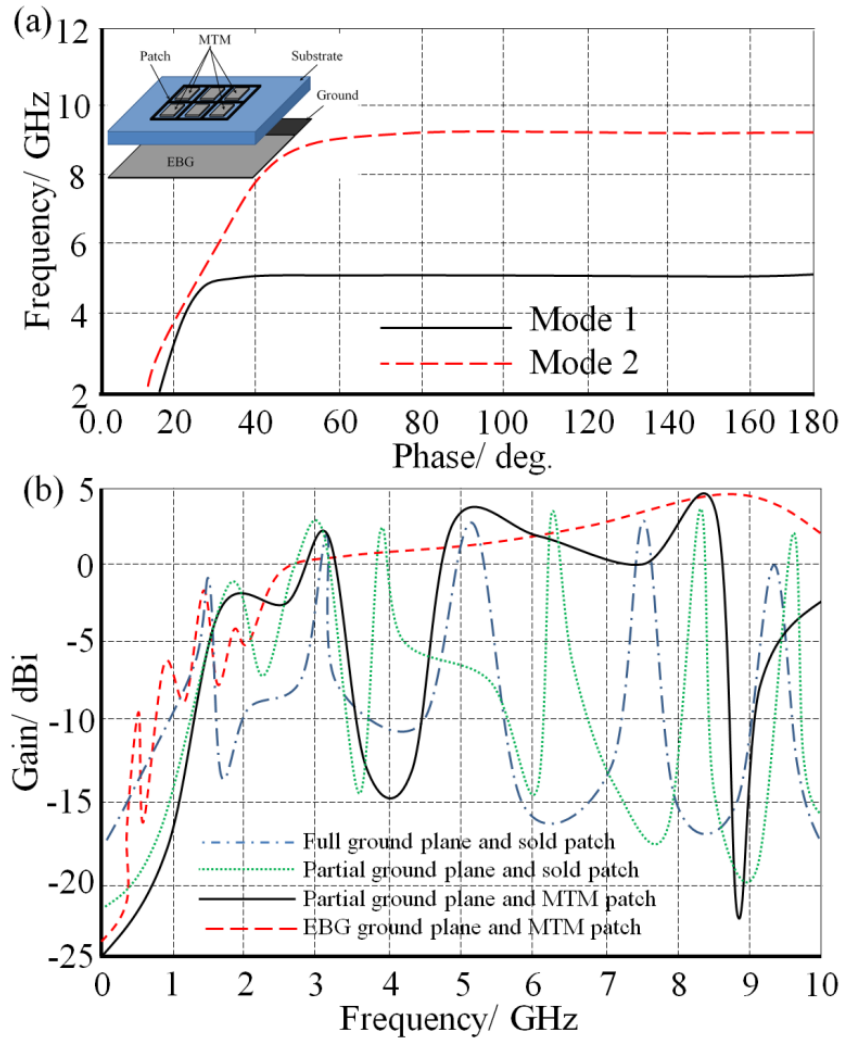

Figure 4.3: Principle of operation; (a) Dispersion diagram and (b) Gain variation.

5. ANTENNA FABRICATION AND MEASUREMENTS

To print the proposed antenna structure, the INP substrate is placed on heated vacuumed stage of 2800 Dimatix material printer. The printer cartridge of 10 pl nominal drop volume is used with heated piezo-electric controller head of 4 jets. A potential difference of 20mV is applied on the piezo-driven jetting device for printing five layers of SNP with 60^{o}C dropping process at 0.5mm height from the substrate. The time delay between each two consecutive printout is 20 seconds. After that, an annealing process is conducted inside ProtoFlow LPKF's convection oven for 10 hours with 120^{o}C after connecting 50Ω SMA port using silver paste to result a printout in Figure 5.1.

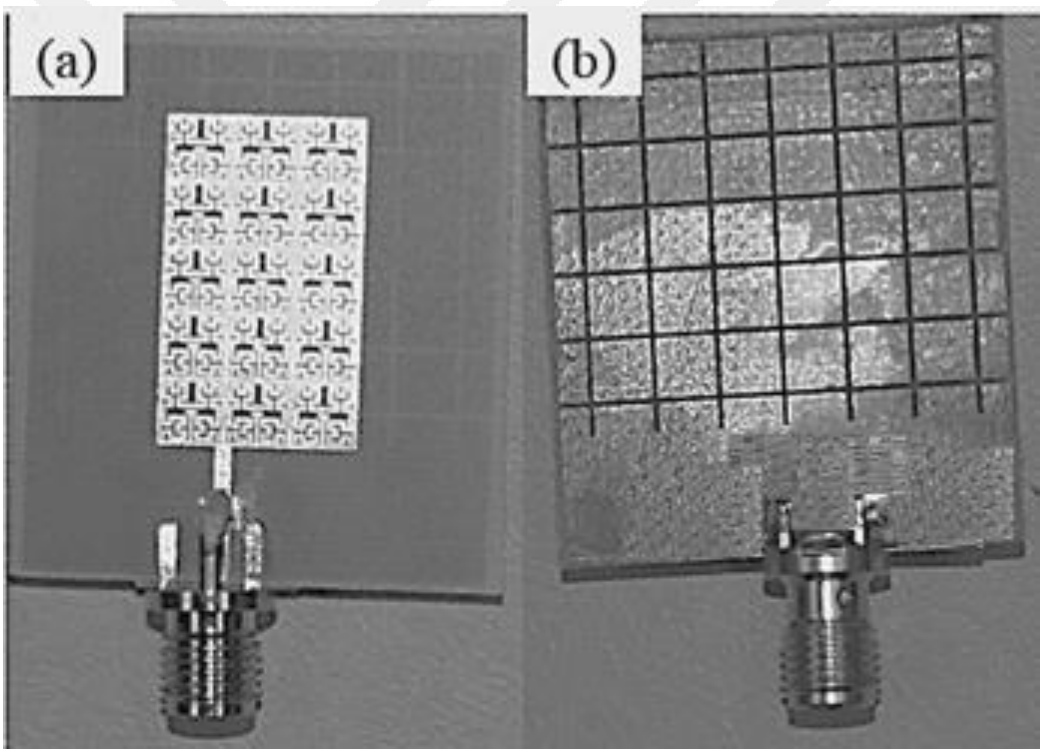

Figure 5.1: Fabricated prototype; (a) Front view and (b) Back view.

Now, the proposed antenna performances based on the evaluated substrate properties and the SNP printout are evaluated inside CSTMWS numerical software package. The fabricated prototype is measured and compared against the simulated results as depicted in Figure 5.2 in terms of S_{11}, gain (G_o), and axial ratio (AR), and e_r response. Therefore, it is observed that the proposed antenna shows an AR below 3dB over a wide frequency range that qualifies the antenna as an excellent candidate for circular polarization in the range from 3.5GH to 7.2GHz. This enhances the ability of the proposed antenna to receive the RF energy with independent of polarization from all directions [12]. As mentioned later, the proposed design was inspired from [19]. However, in this work, the AR is enhanced to be circularly polarized due to using the INP substrate with μr>1 that magnified the magnetic field intensity to circulate the current motion on the patch structure [10]. On the other side, the antenna matching impedance within this band is found to be -10dB and radiation efficiency higher than 80% with excellent gain. All these observation motivated the authors to conduct the next antenna test in terms of radiation measurements and conversion efficiency (η_c) to the proposed antenna with this frequency band.

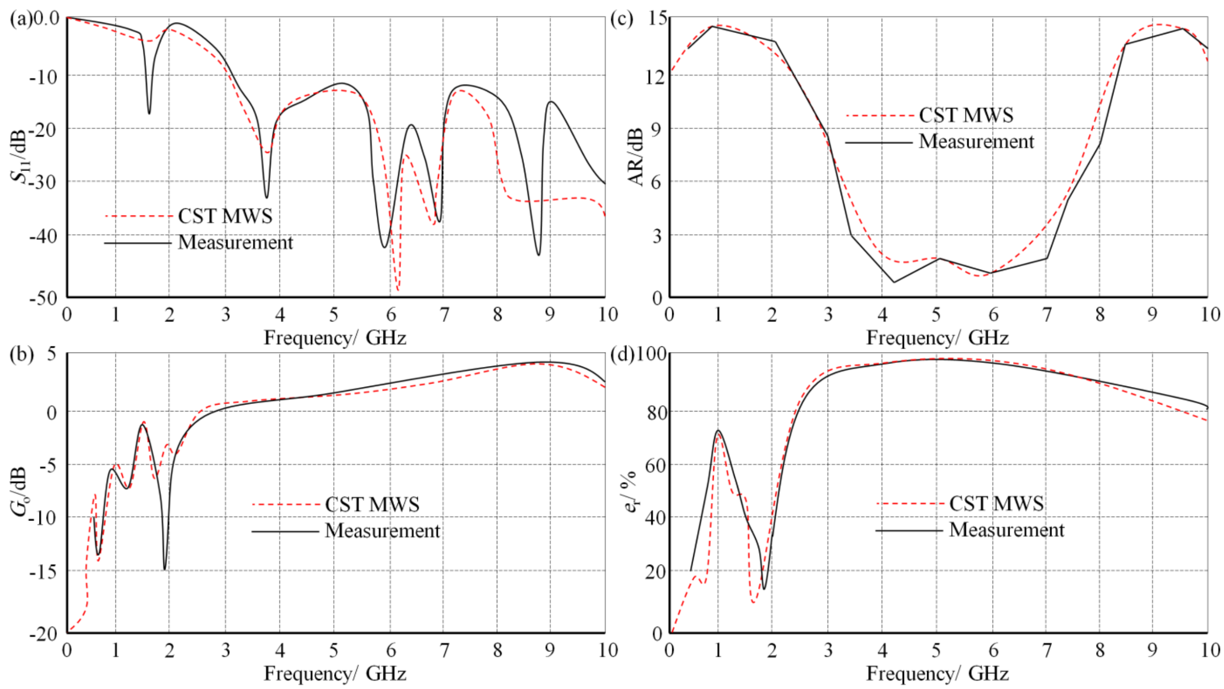

Figure 5.2: Antenna performance results versus frequency; (a) S_{11}, (b) G_o, (c) AR, and (d) e_r.

The antenna radiation patterns are measured at 3.5GHz, 4.2GHz, 5.4GHz, and 6GHz based on their co- and cross-polarizations in the *E*- and *H*-planes as seen in Figure 5.3. It is found that the proposed antenna shows omni directional patterns at the frequency bands of interest which satisfies the requirements of RF harvesting [12].

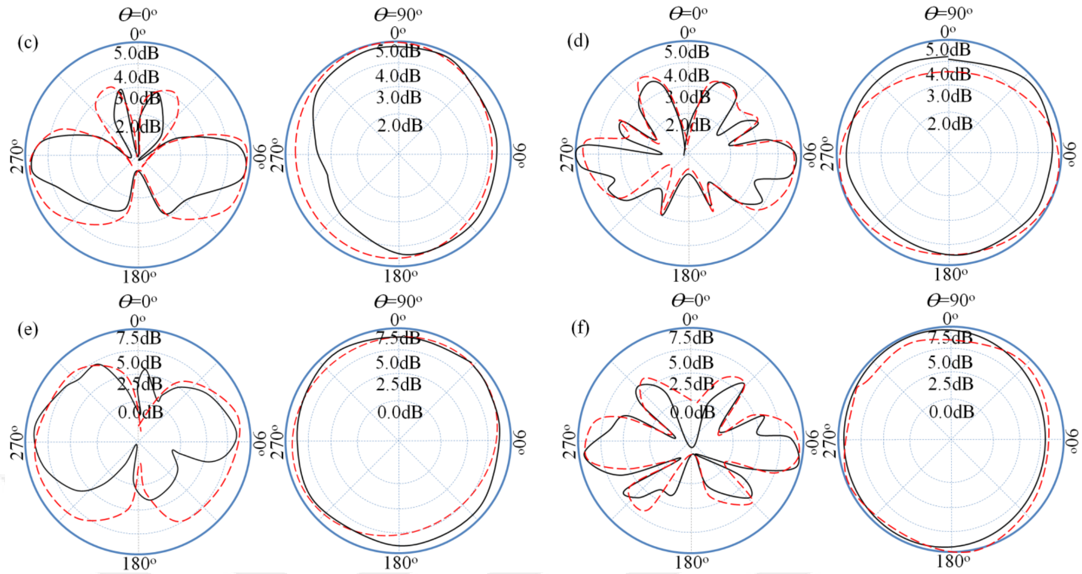

Figure 5.3: Antenna radiation patterns; (a) 3.5GHz, (b) 4.2GHz, (c) 5.4GHz, and (d) 6GHz.

Now, the harvested RF energy performance in terms of η_c at 3.5GHz, 4.2GHz, 5.4GHz, and 6GHz is tested for the proposed antenna. The proposed antenna is connected through an SMA port with 50Ω to an RFD102A test board. The measured η_c responses are realized using an UWB standard horn antenna that covers the entire band of inters. The obtained η_c responses are presented in Figure 5.4 for the proposed antenna. Therefore, the measurements are conducted after considering the antenna in two scenarios as a flat structure and bent structure to test the flexibility effects on the harvesting performance. It is found that η_c at 3.5GHz reaches the maximum enhancement up to 83% for the flat case of proposed antenna. However, when the antenna is bent over on the patch length, the enhancement is dropped insignificantly to be 81% for 5.4GHz. It is very important to mention that the conversion efficiency is calculated relative to the transmitter source power variation from -20dBm to 30dBm. Generally, the enhancement in η_c is attributed to μ_r component of the INP substrate that reduces the surface wave diffractions from the substrate edges. It is good to mention that η_c at all frequencies of interest are obtained from measurements in open field environments according to the recommendations in [19]. Therefore, the obtained η_c can be calculated from the measured results according to the following equation [16]:

$$\eta_c = \frac{V_{DC}^2/R_{out}}{P_{RF}} \tag{5.1}$$

where, P_{RF} is the transmitted RF power from the used horn antenna, V_{DC} is the monitored output DC voltage from the rectifier module on the oscilloscope, and R_{out} is the rectifier module output resistance which is 50Ω.

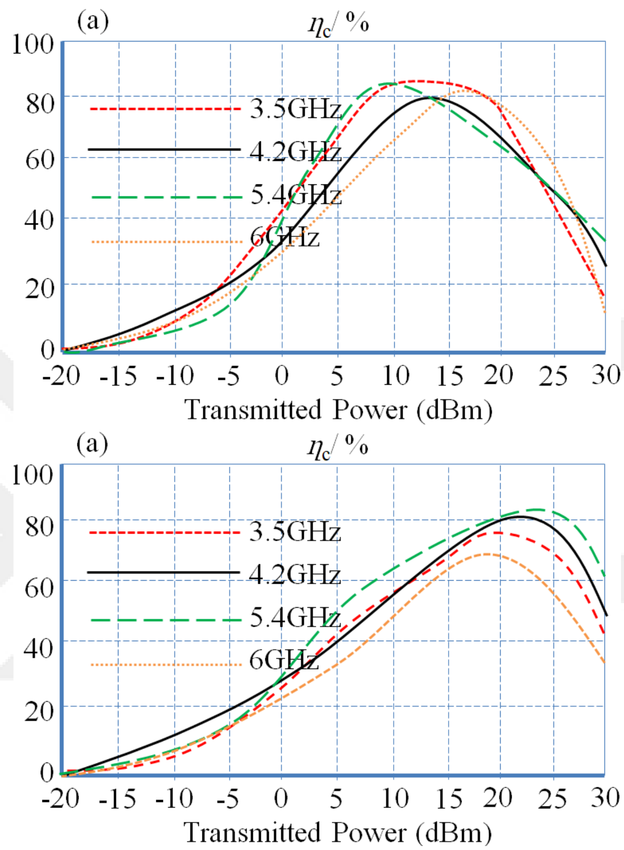

Figure 5.4: η_c measurements at 3.5GHz, 4.2GHz, 5.4GHz, and 6GHz; (a) flat and (b) bent.

Finally, the authors summarized their achievements from the proposed antenna based INP substrate with respect to other published work to provide the achieved advancements. It is found that only the proposed work provided a full study on the effects of bending on harvesting efficiency at different frequencies. Moreover, the used INP mixture supported the proposed design to achieve circularly polarized antenna with a pure resistive part of 50Ω from 3GHz up to 10GHz for the matching impedance. The proposed antenna in this work conducted the use of a microstrip line to provide a circular polarization, while, the proposed design in [21] used a coplanar waveguide to achieve a linear polarization. For this, the proposed work shows a property of harvesting with independent of polarization which is not found in the antenna design in [22]. Table 5.1 shows the comparison of the proposed antenna performance with respect to the published results.

Table 5.1: The proposed work performance comparison with other published results.

Ref.	BW/GHz	Max. Gain/ dBi	Size/ mm^2	Frequencies/ GHz	η_c/ %	η_c after bending/ %	Polarization
14	1	4	10×28	18.8	42	Not applied	Linear
15	0.67	3	10×25	12	41	Not applied	Linear
20	2.4-10	3.4	32×28	2.45, 5.8	78, 88	Not applied	Linear
23	0.08	2	100×2	0.868, 0.915	56,70	Not applied	Circular
24	0.09	0.5	96×14	0.9	30	Not applied	Linear
25	---	1.9	54×2	2.45	44	Not applied	Linear
26	---	6.3	34×23	2.45	38.6	Not applied	Linear
27	1.2–5	4.5	58×55	5	30	Not applied	Linear
28	---	---	1000×4	0.915	80	Not applied	Circular
29	---	-1.54	33×37	2.44	5.	Not applied	Circular
30	1.83-3.58, 5.4-6	4.2	47×46.75	5.8	27.725	Not applied	Linear
31	---	3	35.5×30	2.45	59.5	Not applied	Linear
32	---	4.7	80×71	2.45	33	Not applied	Linear
33	0.02	5.14	120×100	2.4	80	Not applied	Linear
34	1-3	8.89	60×83	2.45	50	Not applied	Circular
This work	3-10	4.6	36×22	3.5, 4.2, 5.4, 6	84, 80, 83, 82	78, 80, 81, 74	Circular

It is good to mention that the proposed work is measured using a VNA of Agilemt Family of 56788BX series with two ports of 50 Ohm coaxial flexible cables. The VNA is interfaced to personal computer with windows 10 through a GPIA cable. This setup is used to measure the antenna S-parameters as seen in Fig. 5.5(a). The antenna radiation patterns are measured respectively inside an RF chamber when the antenna under test is mounted on rotating table as seen in Fig. 5.5(b)

Figure measurement **5.5:** The setup: (a) VNA and (b) RF chamber

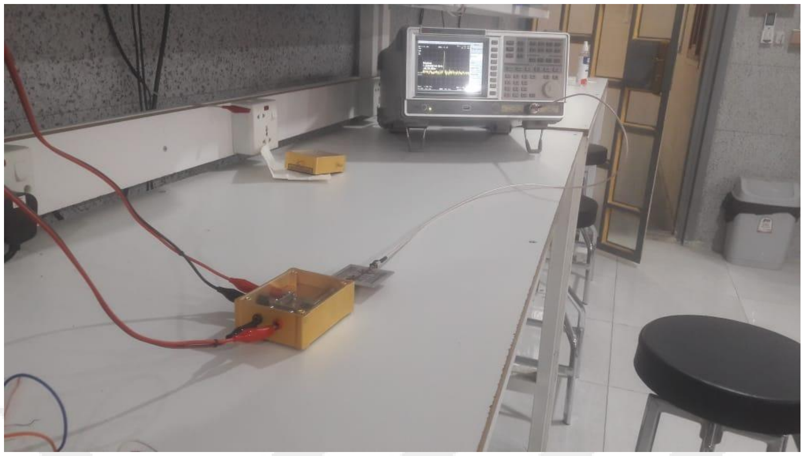

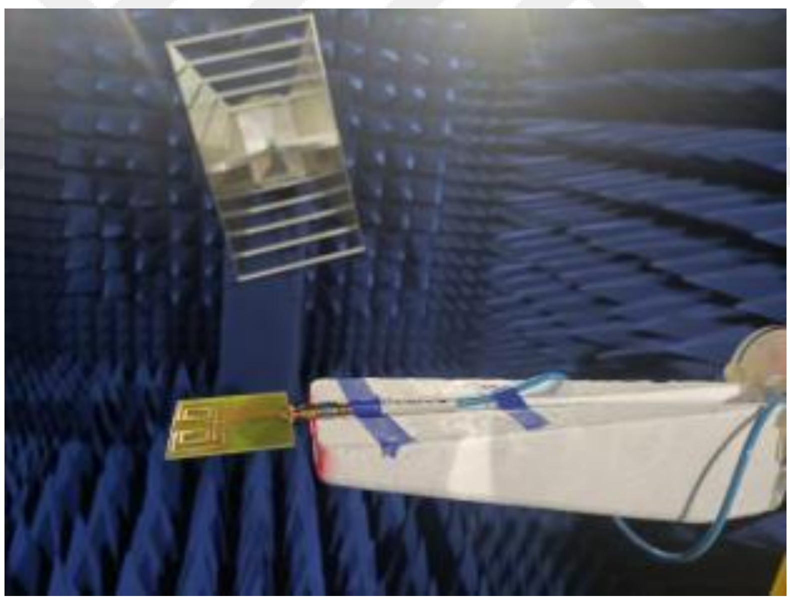

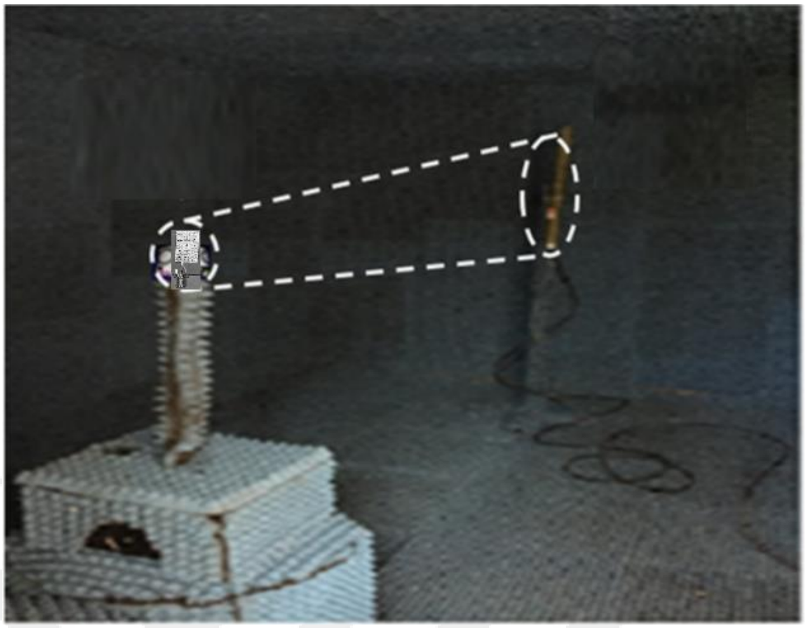

Figure 5.5: The measurement setup: (a) VNA and (b) RF chamber(continued)

The antenna is fabricated using printing process using Dimatix Fujifilm material printer as shown in Fig. 5.6(a). The substrate is treated using plasma surface reactor that is shown in Fig. 5.6(b)

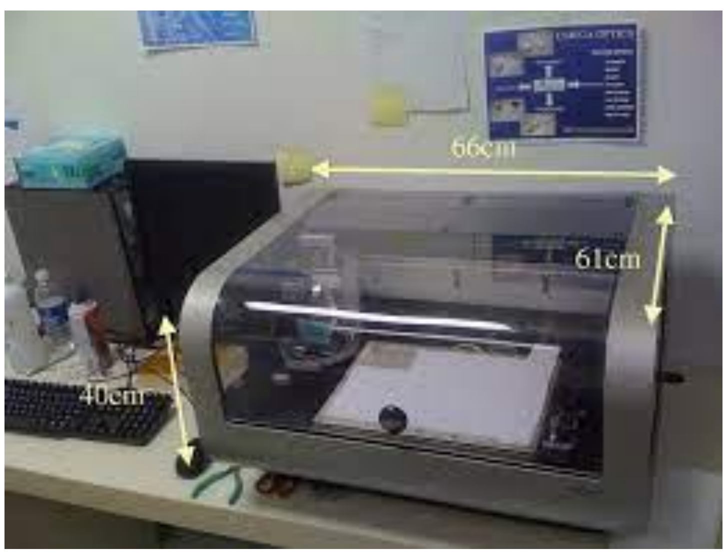

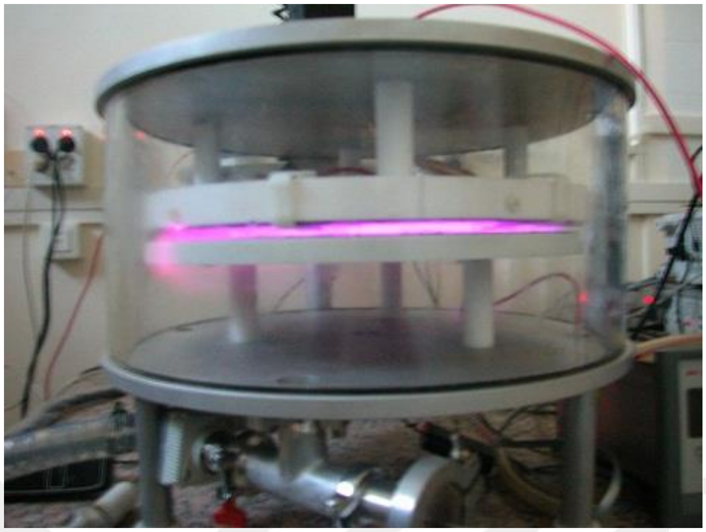

Figure 5.6: The fabrication setup: (a) Material printer and (b) as a plasma reactor.

6. CONCLUSION

In this work, an UWB antenna of MTM circuitry with a miniaturized profile MTM of circularly polarized enhanced gain performances is proposed. Nevertheless, an extensive study of characterization the electromagnetic properties of the INP substrates and the process of the printing process based on KNN algorithm were proposed. The outfit of this study is used to print the antenna on it to provide a flexible structure for smart clothes and wearable applications. The MTM is introduced to realize bandwidth gain product magnification when placed on a flexible INP substrate of defected ground planes. Such enhancement is attributed to the effects of interaction between the proposed MTM and μ_r component of the INP substrate as validated by the experimental measurements. Nevertheless, the proposed antenna is found to show an AR less than 3dB over the measured frequencies at 3.5GHz, 4.2GHz, 5.4GHz, and 6GHz. Therefore, the authors extended the measurements to evaluate the harvesting conversion efficiency at the mentioned frequency bands. In such measurements, the antenna is applied to the bending effects to compare the obtained conversion efficiency for the flat case prototype. The obtained conversion efficiency for the flat case is found about 84% at 3.5GHz, 80% at 4.2GHz, 83% at 5.4, and 82% at 6GHz. While, the maximum output conversion efficiency after bending is found about 78%, 80%, 81%, and 74% at 3.5GHz, 4.2GHz, 5.4GHz, and 6GHz, respectively. The obtained results from both cases reveal insignificant effect on the conversion efficiency due to the enhanced electromagnetic properties of the INP substrate that is described by μ_r. Finally, as a part of future work, the proposed study could be subjected for biomedical applications including wearable and implantable systems. Nevertheless, the proposed work will be extended for harvesting the RF energy over the other frequency bands with different scenarios including bended and flat structures.

In this work the author has used the study to construct a printed circuit antenna for RF harvesting at UWB, however, there are many future works that could be considered in future research as follows:

a. The proposed design is based on the INP substrate. However; as a future study, the author is visited to try to read from a flexible solar panel to provide a dual charging source.

b. The antenna is constructed using a SNP layer printed on the INP substrate; however, the subject of future research is the use of printing technology based on a specific nanoscale process based on the obvious ink to make the proposed antenna.
c. The author has used a third frame of the fractal structure; therefore, the subject of this future study is to apply other orders.
d. The antenna is fitted with a quarter-length transformer to provide the most consistent impedance; therefore, in the future another transformer will be used for this design.
e. Circuit adapter design will be done in antenna design in the next lesson.

The antenna is designed to provide two frequency bands with circular separation; however, the author wishes to in the future expand the antenna design to provide a band-wide band corresponding to the bandwidth over multiple wave bands.

7. REFERENCES

[1] Nguyen, N. H., Bui, T. D., and Le, A. D., “A novel wideband circularly polarized antenna for RF energy harvesting in wireless sensor nodes, ”International Journal of Antennas and Propagation, vol. 2018, Article ID 1692018, 9 pages, 2018.

[2] K. Shafique, B. A. Khawaja, M. D. Khurram et al., “Energy harvesting using a low-cost rectenna for internet of things (IoT) applications,” IEEE Access, vol. 6, pp. 30932–30941, 2018.

[3] D. Nalin, K. Jayakody, S. K. Sharma, and S. Chatzinotas, “Wireless Information and Power Transfer: A New Paradigm for Green Communications,” Springer International Publishing, March 2018.

[4] Al-Janabi, M. A. and Kayhan, S. K., "Flexible Vivaldi Antenna Based on a Fractal Design for RF-Energy Harvesting," Progress In Electromagnetics Research M, Vol. 97, 177-188, 2020.

[5] T. A. Elwi, “A Miniaturized Folded Antenna Array for MIMO Applications”, Wireless Personal Communications, volume 98, issue 2, January 2018.

[6] T. A. Elwi, “Electromagnetic Band Gap Structures based an Ultra-Wideband Microstrip Antenna”, Microwave and Optical Letters, volume 59, issue 4, pp. 827-834, February 2017.

[7] T. A. Elwi, M. A. Rasheed, L. W., Anber, and M. Q. Fahad, “Gain enhancement of a miniaturized inverted λ-dipole antenna,” IEEE ICICT19 International Conference for Information and Communication Technology, April, 2019.

[8] Z. Al-Dulaimi, T. A. Elwi, and D. C. Atilla, “Design of a Meander Line Monopole Antenna Array Based Hilbert-Shaped Reject Band Structure for MIMO Applications,” IETE Journal of Research, Volume 66, issue 1, pp. 1-10, March 2020.

[9] H. M. Al-Sabbagh, T. A. Elwi, Y. Al-Naiemy, and H. M. Al-Rizzo, “A Compact Triple-Band Metamaterial-Inspired Antenna for Wearable Applications”, Microwave and Optical Technology Letters, Volume 11, number 2, October 2019.

[10] T. A. Elwi, “Printed Microwave Metamaterial-Antenna Circuitries on Nickel Oxide Polymerized Palm Fiber Substrates,” Nature Scientific Reports, volume 9, number 2174, pp. 1-14, January 2019.

[11] T. A. Elwi and B. A. Ahmed, “A Fractal Metamaterial based Printed Dipoles on a Nickel Oxide

Polymer Palm Fiber Substrate for Wi-Fi Applications”, AEU - International Journal of Electronics and Communications, volume 96, pp. 122-129, September 2018.

[12] T. A. Elwi, “Metamaterial based a printed monopole antenna for sensing applications”, International Journal of RF and Microwave Computer-Aided Engineering, issue 7, volume 28, September 2018.

[13] A. I. Imran and T. A. Elwi, “A Cylindrical Wideband Slotted Patch Antenna Loaded with Frequency Selective Surface for MRI Applications”, Engineering Science and Technology, an International Journal, volume 20, issue 3, pp. 990–996, April 2017.

[14] A. Takacs, H. Aubert, S. Fredon, L. Despoisse, H. Blondeaux, “Microwave power harvesting for satellite health monitoring,” IEEE Trans. Microw. Theory Tech. volume 62, no. 4, pp. 1090–1098, Mar. 2014.

[15] A. Okba, A. Takacs, and H. Aubert, “Compact flat dipole rectenna for IoT applications,” Progress In Electromagnetics Research C, vol. 87, pp. 39–49, 2018.

[16] T. A. Elwi, O.-A. Tawfeeq, Y. Alnaiemy, H. S. Ahmed, N. Lajos, “An UWB Monopole Antenna Design based RF Energy Harvesting Technology,” IEEE 3rd Scientific Conference of Electrical Engineering SCEE 2018, December, 2018.

[17] T. A. Elwi and A. M. Al-Saegh, “Further realization of a flexible metamaterial based antenna on indium nickel oxide polymerized palm fiber substrates for RF energy harvesting”, International Journal of Microwave and Wireless Technologies, Cambridge, Volume 5, issue 4, pp. 1-9, May 2020.

[18] T. A. Elwi, D. A. Jassim, H. H. Mohammed, “Novel miniaturized folded UWB microstrip antenna-based metamaterial for RF energy harvesting,” International Journal of Communication Systems, Volume 1, issue 2, January 2020.

[19] T. A. Elwi, Z. A. AL-Hussain, O. Tawfeeq, “Hilbert Metamaterial Printed Antenna based on Organic Substrates for Energy Harvesting”, IET Microwaves, Antennas & Propagation, volume 12, number 4, pp.1-8, June 2019.

[20] T. A. Elwi, “Novel UWB Printed Metamaterial Microstrip Antenna based Organic Substrates for RF-Energy Harvesting Applications,” AEU - International Journal of Electronics and Communications, volume 101, pp. 1-10, January, 2019.

[21] S. M. Obaid, T. A. Elwi, and M. Ilyas, “Fractal Minkowski-Shaped Resonator for Noninvasive Biomedical Measurements Blood Glucose Test,” *Progress in Electromagnetics Research c*, Volume 107, pp. 143-156, December 2020.

[22] T. A. Elwi, “Further Investigation on Solant-Rectenna based Flexible Hilbert-Shaped Metamaterials”, *IET Nanodielectrics*, Volume 4, issue 12, pp. 1-12, March 2020.

[23] S. wang and Y. Song; “A compact A compact wideband helix antenna for wireless meat probe with highly efficient RF energy harvesting,” IEEE 2019, Cross Strait Quad-Regional Radio Science and Wireless Technology Conference (CSQRWC).

[24] N. Rezazadeh and L. Shafai, A Pattern Diversity Antenna for Ambient RF Energy Harvesting in Multipath Environment, IEEE 2018 18th International Symposium on Antenna Technology and Applied Electromagnetics (ANTEM).

[25] A. Desai and P. Nayeri, “A multilinear polarization reconfigurable plus shaped dipole antenna for wireless energy harvesting applications,” IEEE 2018 International Applied Computational Electromagnetics Society Symposium (ACES).

[26] A. Okba; A. Takacs; hervé AUBERT, “Compact Flat Dipole rectenna for energy Harvesting or Wireless Power Transmission applications”, 2018 IEEE International Symposium on Antennas and Propagation & USNC/URSI National Radio Science Meeting.

[27] M. Mansour, X. Le Polozec and H. Kanaya, “Enhanced Broadband RF Differential Rectifier Integrated with Archimedean Spiral Antenna for Wireless Energy Harvesting Applications,” Sensors 2019, 19, 655; doi:10.3390/s19030655.

[28] H. Lyu, X. Liu, Y. Sun, Z. Jian, and A. Babakhani, “A 915-MHz Far-Field Energy Harvester With −22-dBm Sensitivity and 3-V Output Voltage Based on Antenna-and- Rectifier Codesign,” IEEE MICROWAVE AND WIRELESS COMPONENTS LETTERS, VOL. 29, NO. 8, AUGUST 2019.

[29] R. L. Shao, B. Li, L. Yang, Y. J. Zhou, “Electrically small multiband antenna based on spoof localized surface plasmons,” EPJ Appl. Metamat. 6, 11 (2019).

[30] O. M. A. Dardeer, H. A. Elsadek, and E. A. Abdallah, “Compact Broadband Rectenna for Harvesting RF Energy in WLAN and WiMAX Applications,” 2019 International Conference on Innovative Trends in Computer Engineering (ITCE’2019), Aswan, Egypt, 2-4 February 2019.

[31] M. M. Mansour and H. Kanaya, “Novel L-Slot Matching Circuit Integrated with Circularly Polarized Rectenna for Wireless Energy Harvesting,” Electronics 2019, 8, 651.

[32] Krishnamoorthy, K. Umapathy, “Design And Implementation Of Microstrip Antenna For Energy Harvesting Charging Low Power Devices,” IEEE 4th International Conference on Advances in Electrical, Electronics, Information, Communication and BioInformatics (AEEICB-18).

[33] V. S. Sankar, R. Kumari, B. Choudhury, “Metamaterial-Inspired Rectenna Loaded With a DR for RF Energy Harvesting,” 2018 IEEE Indian Conference on Antennas and Propogation (InCAP).

[34] M. M. Mansou; O. Takiguchi; T. Inoi; H. Kanaya, “Experimental investigation of wireless energy harvesting with a Bluetooth low energy sensing unit”; 2018 International Conference on Electronics Packaging and iMAPS All Asia Conference (ICEP-IAAC).